

Research

Deciphering the interaction between the expression of LRP2 served as a mitochondrial metabolism-related gene and prognosis in colon cancer integrating multi-omics analysis

Jie Zhang¹ · Ziyun Liu² · Xiaoqing Ma² · Zhenyu Shi³ · Jing Zhao³ · Yongjie Xie² · Xiaobin Shang^{4,5} · Xia Zhang³

Received: 5 November 2024 / Accepted: 5 May 2025

Published online: 16 May 2025

© The Author(s) 2025 **OPEN**

Abstract

Background Colon adenocarcinoma (COAD) is increasingly prevalent among patients under 50 years old, and the 5-year survival rate for patients with metastasis is less than 20%. Identifying significant biomarkers and therapeutic targets is crucial. We investigated the expression of LRP2 in COAD and its prognostic value utilizing single-cell sequencing and transcriptomics datasets, which was conducted preliminary validation at the patient samples and cellular levels as well. **Methods** Based on differential gene expression of tumor samples and normal tissues in The Cancer Genome Atlas (TCGA), we performed consensus clustering, univariate and multivariate Cox regression analysis applying 1,234 mitochondrial metabolism-related genes (MMRGs) to identify some essential genes associated with poor prognosis in COAD patients. We validated survival outcome and biological function of the target gene leveraging single-cell sequencing and transcriptomics datasets from Gene Expression Omnibus (GEO), and evaluated the value of the target gene in the clinical pathology stage of COAD patients. Simultaneously, the expression levels of critical gene were detected in the diverse tissues of COAD by immunohistochemistry (IHC) staining. Transcriptomics data was continuously implemented to compare the discrepancy between the expression levels of the target gene and somatic mutation burden, inspecting the key pathways of the target gene by gene set enrichment analysis (GSEA) and examining its drug sensitivity synthetically in the CellMiner databases. The proliferative capacity augmented in LRP2-overexpressed colon cancer cells was determined employing cell counting kit-8 (CCK-8) and flow cytometry assays.

Jie Zhang, Ziyun Liu and Xiaoqing Ma have contributed equally.

Supplementary Information The online version contains supplementary material available at <https://doi.org/10.1007/s12672-025-02568-2>.

✉ Yongjie Xie, 2335940013@qq.com; ✉ Xiaobin Shang, shangxiaobin@tmu.edu.cn; shangxiaobin626@live.cn; ✉ Xia Zhang, zhangxia864@126.com; Jie Zhang, zhangjaysiwei@163.com; Ziyun Liu, liuziyun0115@tmu.edu.cn; Xiaoqing Ma, maxiaoqing0806@163.com; Zhenyu Shi, shizhenyu_915@163.com; Jing Zhao, zhj.82@163.com | ¹Tianjin Medical University Cancer Institute and Hospital, National Clinical Research Center for Cancer, Key Laboratory of Cancer Prevention and Therapy, Tianjin's Clinical Research Center for Cancer, Tianjin Medical University, Tianjin 300060, China. ²Department of Pancreatic Cancer, Tianjin Medical University Cancer Institute and Hospital, National Clinical Research Center for Cancer, Key Laboratory of Cancer Prevention and Therapy, Tianjin's Clinical Research Center for Cancer, Tianjin 300060, China. ³Department of Biochemistry and Molecular Biology, Tianjin Medical University Cancer Institute and Hospital, National Clinical Research Center for Cancer, Key Laboratory of Cancer Prevention and Therapy, Tianjin's Clinical Research Center for Cancer, Tianjin 300060, China. ⁴Department of Minimally Invasive Esophageal Surgery, Tianjin Medical University Cancer Institute and Hospital, National Clinical Research Center for Cancer, Key Laboratory of Cancer Prevention and Therapy, Tianjin's Clinical Research Center for Cancer, Tianjin 300060, China. ⁵ Department of Thoracic Surgery, National Cancer Center/National Clinical Research Center for Cancer/Cancer Hospital, Chinese Academy of Medical Sciences and Peking Union Medical College, Beijing, 100021, China.



Results LRP2 served as a key mitochondrial metabolism-related gene was assessed clinical prognosis in COAD patients according to the TCGA database. High expression of LRP2 was prominently associated with poor prognosis in COAD patients ($P < 0.05$), which was validated by GEO databases, and the expression levels of LRP2 were positively related to clinical pathological stage simultaneously ($P < 0.05$). Some specific cell types were clustered and proliferation pathways were immensely enriched, which were correlated with LRP2 in two single-cell sequencing datasets. The mutation profiles displayed remarkable differences in two levels of LRP2, we also observed high expressions of LRP2 were immensely correlated with high tumor mutation burden (TMB) and unfavorable prognosis in these patients ($P < 0.05$). LRP2 was significantly enriched in multiple cancer proliferation-related pathways, and the noteworthy correlation between LRP2 and the sensitivity to various drugs was identified ($P < 0.05$). The expression levels of LRP2 were multifarious in different COAD patients based on IHC staining. LRP2-overexpression could stimulate the proliferation capability of HCT116 and SW480 cell lines markedly ($P < 0.05$).

Conclusion The expression levels of LRP2 were intimately correlated with gene mutations, prognosis, pathological stage and the sensitivity to anticancer drugs in COAD. Augmented levels of LRP2 would manifest poor prognosis, which furnished novel insights for clinical diagnosis and treatment in COAD. LRP2 could extensively facilitate the proliferation ability of colon cell lines.

Keywords Colon cancer · Prognosis · LRP2 · Multi-omics · Cell proliferation

1 Introduction

The incidence and mortality rates of colorectal cancer ranked third among cancers and had become the second leading cause of death among cancer patients [1]. Although the incidence and mortality rates of colorectal cancer were slowly declining, the proportion of patients under 50 years old was increasing, with a higher occurrence in the left colon [2]. Approximately 20% of colorectal cancer patients would develop metastasis, and the five-year survival rate was less than 20% [3]. Patients diagnosed with early-stage colon cancer could undergo surgical treatment, but there was a 40% recurrence rate in those with clinical stage III [4]. Therefore, identifying meaningful biomarkers would provide a new perspective for the prognosis assessment and treatment of colon cancer patients.

Tumor cells can alter their metabolic pathways to prompt energy production including metabolic reprogramming to maintain their stable survival and rapid proliferation capability [5]. Mitochondria are crucial bioenergetic hubs for cellular metabolism and responsible for oxidative phosphorylation (OXPHOS), fatty acid oxidation (FAO), tricarboxylic acid (TCA) cycle, and electron transport chain (ETC) processes, all of which may promote the development and maintenance of malignant phenotypes in tumor cells [6]. Dysregulation of mitochondrial metabolic pathways caused by mitochondrial metabolism-related genes may facilitate tumor onset, progression, and immune evasion [7]. However, there was little systematic research that the relevant genes could stimulate mitochondrial metabolic disturbances and concentrate on the risk assessment and targeted therapy for colon carcinoma patients.

Single-cell sequencing and transcriptomics analysis complemented novel insights in colorectal cancer research [8, 9]. With the developments in single-cell technology, we could obtain a deeper understanding of the metabolic abnormalities, tumor microenvironment, and heterogeneity in tumor development and identify personalized therapeutic strategies corresponding with COAD.

In the present study, it had revealed that mitochondrial metabolic pathways participated in accommodating colon cancer progression [10, 11]. By comparing the differential expression of 1,234 mitochondrial metabolism-related genes in colon cancer patients and their prognostic impact, LRP2 was identified as a key gene for assessing the prognosis of colon cancer patients. Simultaneously, we employed single-cell RNA sequencing and microarray datasets from the Gene Expression Omnibus (GEO) and mRNA-seq data from The Cancer Genome Atlas (TCGA) database to explore LRP2 affect COAD metabolic activities.

LRP2 was an endocytic receptor that combined and internalized various ligands, such as vitamin-binding protein complexes [12], lipid transport proteins, protease-inhibitor complexes, hormones, lipoproteins, and lipocalins [13–15]. Previous studies had illustrated that silencing LRP2 could inhibit the proliferation of thyroid cancer cells and reduce the survival rate of melanoma cells [16, 17]. Therefore, it was speculated that LRP2 may be involved in regulating colon cancer occurrence and progression. Conducting multi-omics bioinformatics analysis of the pathway enrichment and drug sensitivity of LRP2 in COAD samples, these results unraveled regulatory mechanisms of LRP2 in the occurrence

and development of colon cancer, and which was preliminarily validated performing immunohistochemical staining and COAD cell experiments. LRP2 certainly enhanced the developmental activity of two colon carcinoma cell lines.

This study provided a theoretical support for exploring the application of mitochondrial metabolism-related genes in the prevention, early diagnosis, and effective treatment of COAD. LRP2 may serve as a novel target for the progression assessment and personalized treatment of colon carcinoma patients.

2 Materials and methods

2.1 Data sources and preprocessing

COAD mRNA-seq data and relevant clinical information (including 476 colon cancer samples and 41 adjacent normal tissues) were obtained from TCGA database. The extensive datasets (single-cell sequencing data: GSE132465 and GSE179784; transcriptome data: GSE39582 and GSE38832) utilized in this study were downloaded from GEO databases, which was employed for verification analysis of the selected gene. In the scRNA-seq datasets, low-quality cells were excluded with mitochondrial genes $\leq 20\%$, UMI ≤ 500 , and gene count $\geq 50,000$. The more significant variance genes were proceeded for downstream analysis. Transcriptome databases were standardized using the $\log_2(X + 1)$ method in R 4.2.3, and differential analysis was performed using the “limma” package to compare colon cancer and normal samples with the cutoff criteria: false discovery rate (FDR) < 0.05 and $|\log_2 \text{fold change (FC)}| > 1$.

2.2 Screening of DEGs associated with mitochondrial metabolism-related and cellular differentiation-related

According to literature report, 1,234 mitochondrial metabolism-related genes (MMRGs) were obtained [18]. Additionally, we distinguished 2,264 cellular differentiation-related genes (CDRGs) from single-cell sequencing datasets. The intersection was taken with expression differences of CDRGs and MMRGs from COAD and adjacent normal tissues. A univariate Cox regression analysis was conducted on the related genes possessed significant prognosis assessment prospects.

2.3 Authentication of molecular subtype characteristics and construction of prognostic model based on MMRGs and CDRGs

Based on these prognostic genes, we inspected the molecular subtype utilizing an unsupervised consensus clustering approach employing the “ConsensusClusterPlus” package, which introduced a K-means clustering algorithm to identify robust clusters, setting the maximum number to 10. The optimal number of clusters was assessed employing the Consensus Matrix and Cumulative Distribution Function (CDF) curves. To further detect critical prognostic signatures, the related genes were analyzed employing least absolute shrinkage and selector operation (LASSO) regression model by “glmnet” package. Subsequently, these identified prognostic genes were used to construct the related gene scores for each COAD sample. The related gene scores were calculated as the following formula: $\text{SMARCD3} \times 0.106 + \text{ACBD4} \times 0.096 + \text{MBOAT1} \times 0.052 + \text{LRP2} \times 0.154 + \text{OSBPL1A} \times 0.060 + \text{PNPLA7} \times 0.167 + \text{RAB6B} \times 0.045 + \text{CYP11A1} \times 0.009 + \text{TNFAIP8L3} \times 0.047 + \text{ALOX12B} \times 0.100 + \text{CHAT} \times 0.056 + \text{SLCO1A2} \times 0.069 + \text{ACSL6} \times -0.025 + \text{PPARGC1A} \times -0.244$. Additionally, the 1-, 3-, and 5-year prediction accuracy of the model was investigated by plotting the receiver operating characteristic (ROC) curves [19]. The differences in Overall Survival (OS) both diverse clusters and models were assessed performing Kaplan Meier survival analysis in TCGA, GSE39582, and GSE38832 datasets.

2.4 Identification of key target signature and gene ontology (GO) enrichment analysis

To further investigate the decisive genes in the predictive model, we conducted a multivariate Cox regression analysis. The target biomarker upregulating in COAD and preforming a high hazard ratio (HR) would be percolated. We validated its significance of clinical prognosis evaluation by incorporating survival information and clinical pathological features from multiple datasets. Furthermore, the single-cell RNA data associated with critical signature was log-normalized and dimensionality was lessened conducting Principal component analysis (PCA), followed by t-distributed stochastic neighbor embedding (t-SNE) and uniform manifold approximation and projection (UMAP) for visualization [20]. We manually annotated Cell types to define distinct cellular populations, focusing on variable epithelial and immune cells.

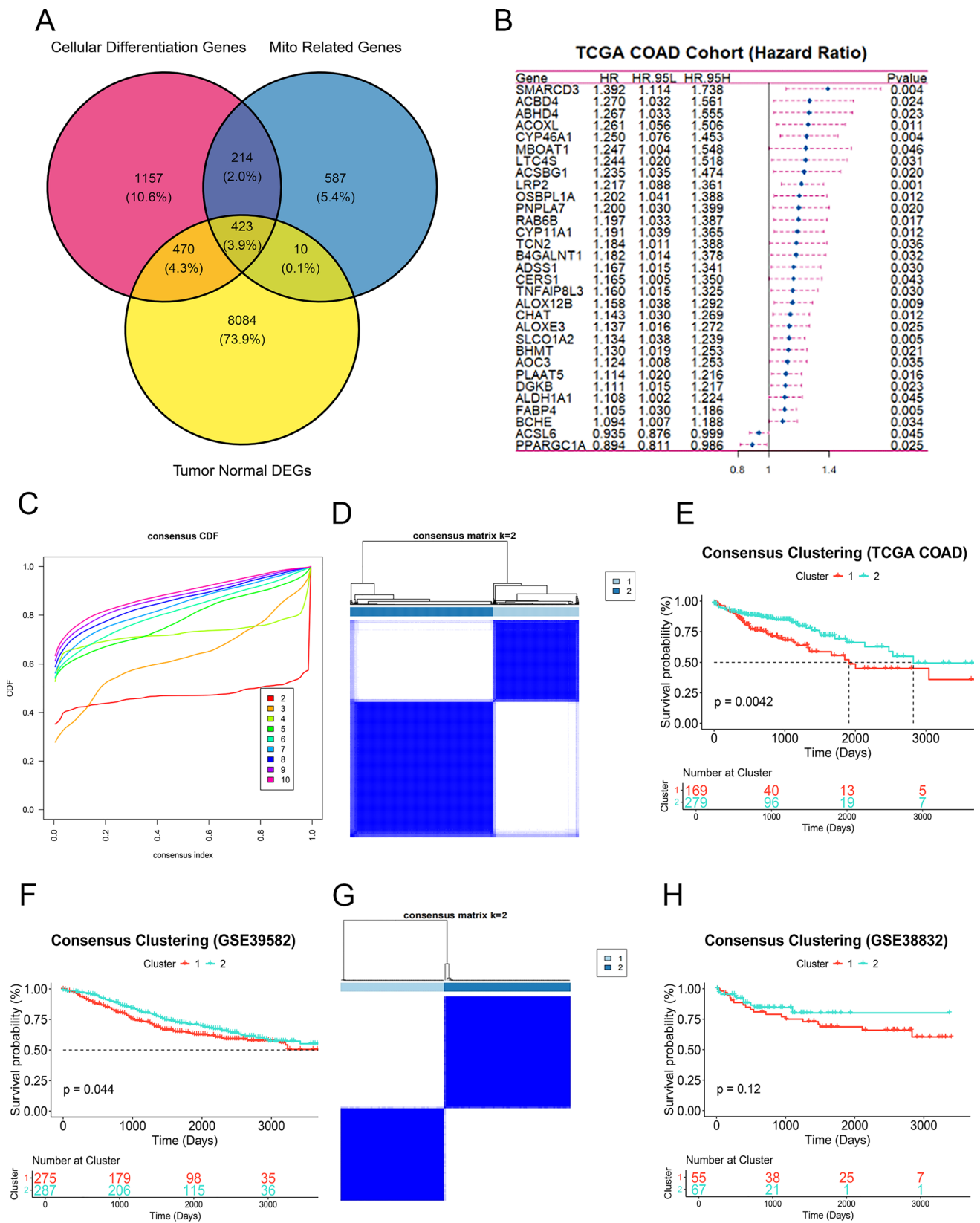


Fig. 1 Screening mitochondrial metabolism-related genes as assured prognostic biomarkers in COAD. **A** Comparison of MMRGs; **B** Examination of 31 critical genes using univariate Cox analysis; **C** The cumulative distribution function curve of MMRGs clustering; **D** Consensus matrices of the TCGA dataset for k= 2; **E** Kaplan–Meier (KM) curves of COAD patients in two different clustering groups; **F** Outcome of COAD patients between cluster 1 and cluster 2 in GSE39582; **G** The consensus matrix of the k-means clustering (k = 2) in GSE38832; **H** Validation for the overall survival (OS) of two different COAD cohorts in GSE38832

With $|\log_2 FC| > 0.585$ and $FDR < 0.05$, differential analysis was performed on different differentiation states. The filtered cell differentiation-related genes relevant with the selective biomarker were implemented GO enrichment analysis to further comprehend the biological significance.

2.5 GSEA analysis

Gene Set Enrichment Analysis (GSEA) was utilized to identify key pathways involving the target gene in the occurrence and development of colon cancer [21]. GSEA analysis was carried out on pathways annotated in Gene Ontology (GO), Kyoto Encyclopedia of Genes and Genomes (KEGG), and HALLMARK. Differential analysis of COAD samples with multifarious risk scores and expression levels of critical genes in TCGA were performed using the “limma” package ($FDR < 0.05$ and $|\log_2 FC| > 1$). The essential pathways related to prognostic signature were sorted by their normalized enrichment scores, selecting pathways with $p < 0.05$ for further analysis.

2.6 Mutation analysis

Somatic mutation data for COAD was acquired from TCGA database. The “maftools” package was used to create waterfall plots to illustrate the mutation landscape for COAD patients of multitudinous expression levels of target gene, calculating the mutation burden score for each sample.

2.7 Drug sensitivity analysis

Integration and analysis of molecular and pharmacological data from the NCI-60 tumor cell lines were conducted in the CellMiner database (www.discover.nci.nih.gov) [22]. Clinical trial and FDA-approved drugs were sieved, and we calculated the Pearson correlation coefficient between the expression of the selected prognostic genes and these drugs, with $P < 0.05$ as the threshold for selection of results utilizing “impute” and “limma” packages.

2.8 Immunohistochemistry (IHC) staining

Target gene was experimentally verified by IHC staining. We collected diverse colon cancer tissue samples to perform IHC staining from Tianjin Medical University Cancer Institute and Hospital. Ethical approval was received from the hospital ethics committee and all patients signed informed consent forms. Two independent pathologists evaluated and scored the immunohistochemical staining. Staining intensity was graded from 0 to 3, with 0 implicating no staining, 1 representing weak staining, 2 implicating moderate staining, and 3 indicating strong staining, separately.

2.9 Cell culturing and lentiviral transfection

Human colon cancer HCT116 and SW480 cell lines were purchased from ATCC and cultivated in DMEM medium supplemented with 10% FBS and 1% penicillin–streptomycin under the condition of 37 °C in a humidified atmosphere ($\geq 95\%$) with 5% CO_2 . The negative control (NC) group and overexpression (LRP2-OE) group were established for constructing empty and LRP2 overexpression lentiviral vectors (Beyotime, China), respectively. The complete culture medium was replaced after 12 h, and the cells were cultured about 72 h continuously until they could be applied for subsequent experiments.

2.10 Real-time quantitative PCR (RT-qPCR)

RT-qPCR was performed to detect the expression of two selected genes: LRP2 and the internal control gene glyceraldehyde-3-phosphate dehydrogenase (GAPDH). RNA was extracted from HCT116 and SW480 cell lines and then cDNA was synthesized using a reverse transcription kit (Takara, Japan). The relative gene expression of LRP2 was assessed based on the $2^{-\Delta\Delta CT}$ method. Primer sequences were as follows: GAPDH Forward: 5'-TAGAGCGCCGCCATGTT-3', Reverse: 5'-CGCCAAATACGACCAAATCAGA-3'; LRP2 Forward: 5'-TTTTGGCCACTAGGAGCTGG-3', Reverse: 5'-CGCACTGTACATTCTTGGC-3'.

Fig. 2 Construction of MMRGs prognostic model for COAD patients. **A** Least absolute shrinkage and optimal coefficient profiles of the selective gene sets; **B** Determination of the number of factors by the LASSO regression analysis; **C–E** Kaplan–Meier curves between high-risk score and low-risk score cohorts in the TCGA (**C**), GSE39582 (**D**), and GSE38832 (**E**) sets; **F** ROC curves indicate the 1-, 3-, 5-years survival of COAD patients in TCGA; **G** GO results related to various risk score groups employing GSEA analysis; **H** KEGG results employing GSEA analysis connected with risk scores

2.11 Western blot

The lysate was separated using SDS-PAGE and then transferred to PVDF membranes. The membranes were washed five times with $1 \times$ TBST, which were then blocked by 5% skimmed milk. They were incubated with primary antibodies for two hours, with antibodies including LRP2 (1:1000, ab313741, Abcam) and GAPDH (1:1000, ab181602, Abcam). The membranes were washed five times with $1 \times$ TBST again and transferred to secondary antibodies for overnight incubation. Protein detection was performed using an ECL reagent (Beyotime, China) on the Tanon-5000 system and gray values were examined by ImageJ software.

2.12 CCK-8 assay for cell viability

Cells in the logarithmic growth phase were selected and seeded into a 96-well plate at a density of 2,000 cells/well. After being cultured for 0, 24, 48, 72, and 96 h, cell lines were added by the CCK-8 reagent and incubated at 37°C with 5% CO_2 for 2 h. The optical density (OD) was measured at a wavelength of 450 nm.

2.13 Flow cytometry

Logarithmic phase cells were seeded into 6-well plates at a density of 5×10^5 cells/well and continued to culture about 48 h. The cell suspension was collected and subsequently treated with APC-EdU and FITC-Ki67 for 30 min in the dark at room temperature. Flow cytometry was used to detect cell proliferation activity.

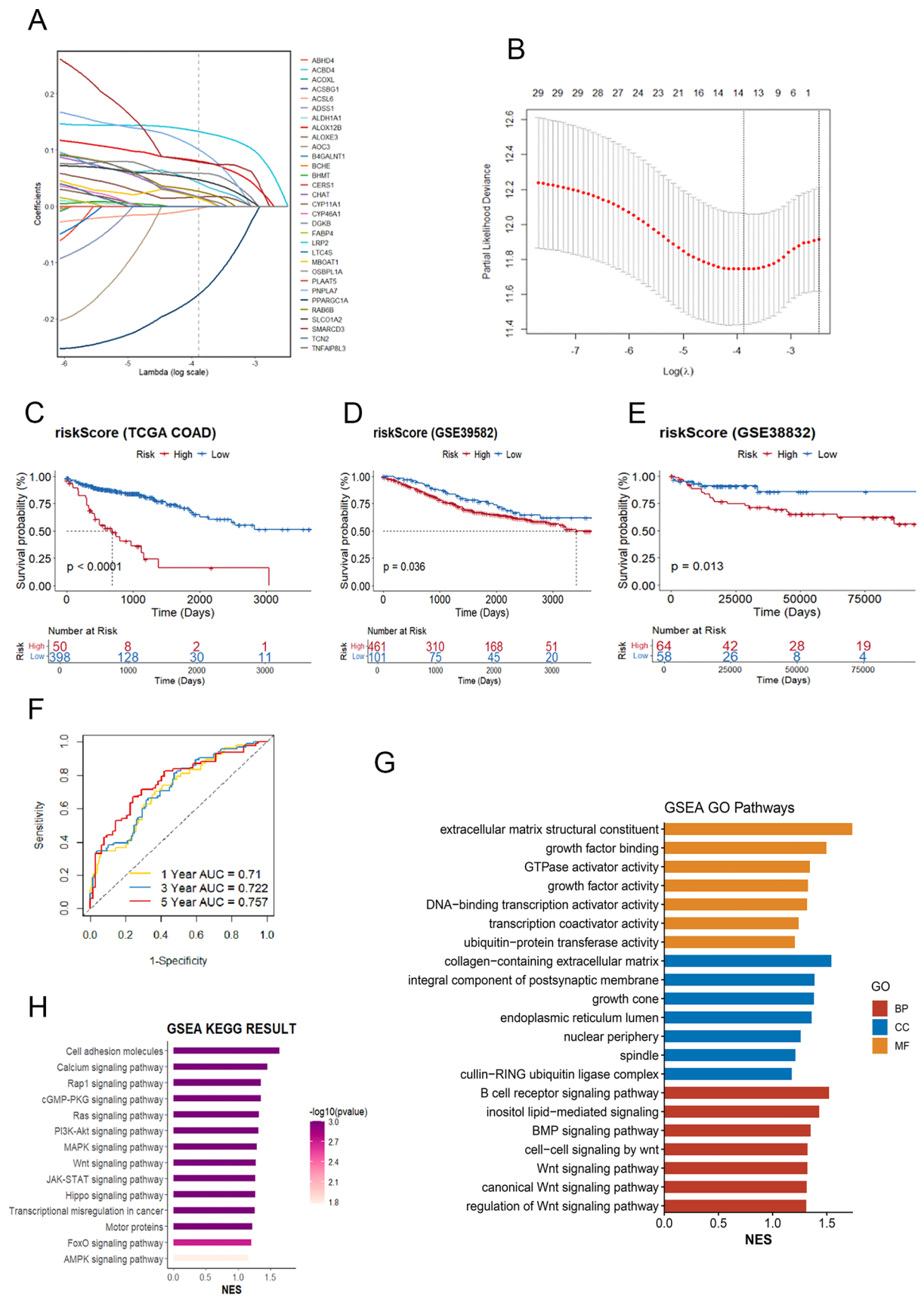
3 Results

3.1 Identification of mitochondrial metabolism-related and cellular differentiation-related clusters in COAD

This study was performed to identify mitochondrial metabolism-related genes associated with colon cancer prognosis and to further investigate their roles in the progress of COAD. A comparison of differential expression in colon cancer samples and adjacent tissues yielded 8,987 differential genes (including 1,467 upregulated genes and 7,520 downregulated genes) (Fig. S1 A). The intersection of 1,234 mitochondrial metabolism-related genes with the 8,987 differential genes and 2266 cellular differentiation-related genes produced 423 common genes (Fig. 1A). Univariate Cox analysis identified 31 genes significantly associated with prognosis ($P < 0.05$) (Fig. 1B). We conducted consensus clustering analysis in 476 COAD patients from the TCGA database, through clusters (K) from 2 to 10. When $k = 2$, the optimal grouping was strongly determined on the expression matrix of 31 related genes in the training cohorts (TCGA-COAD) (Fig. 1C, D and S1B, C). Compared with cluster 2, the shorter survival time of cluster 1 indicated a worse outcome ($P < 0.05$) (Fig. 1E). The same result was further validated in the GSE39582 dataset ($P < 0.05$) (Fig. 1F and S1D). The intragroup correlation was fierce at $k = 2$ and cluster 1 owned a poorer prognosis in the GSE38832 database (Fig. 1G, H).

3.2 Estimation of the potential elements

To screen critical signatures, we operated LASSO logistic regression to identify 14 biomarkers, including SMARCD3, ACBD4, MBOAT1, LRP2, OSBPL1A, PNPLA7, RAB6B, CYP11A1, TNFAIP8L3, ALOX12B, CHAT, SLCO1A2, ACSL6, PPARGC1A (Fig. 2A, B). The expression heatmap of 14 genes between tumor samples and normal tissues represented a prominent distinction (Fig. S1E). It divided different colon cancer patients into two groups. Compared with the low-risk group, more deaths and shorter survival time of the COAD patients with the high risk were observed simultaneously in TCGA ($P < 0.0001$), GSE39582 ($P = 0.036$), and GSE38832 ($P = 0.013$) datasets (Fig. 2C–E). Next, the predictive value of the prognostic



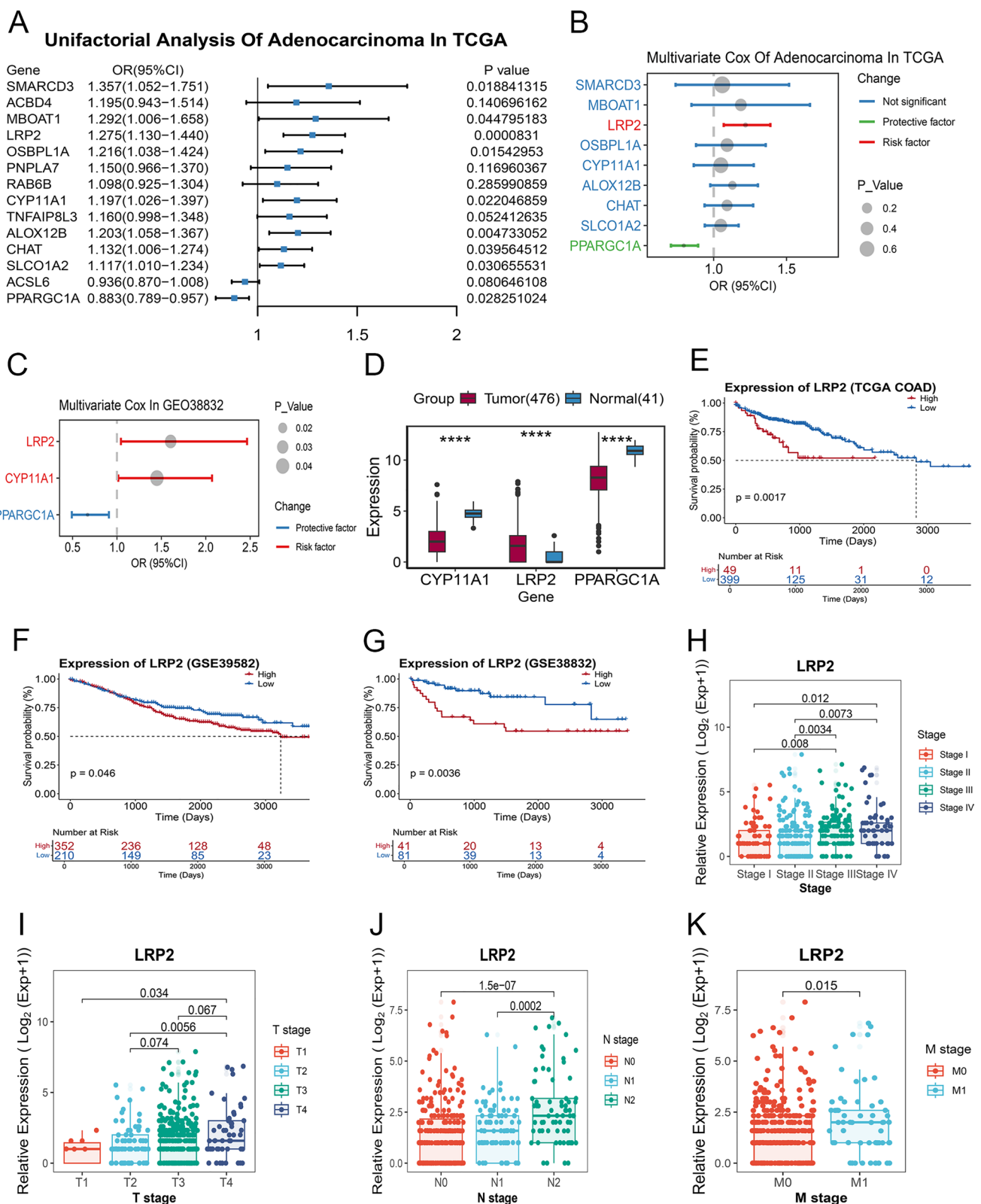


Fig. 3 LRP2 was sieved from prognostic biomarkers of COAD patients. **A** 9 potential biomarkers were further selected from 14 biomarkers ($P < 0.05$); **B** The results of multivariate cox analysis of 9 markers in TCGA; **C** The results of multivariate cox analysis of 3 markers in GEO38832; **D** Expression levels of 3 candidate genes between tumor samples and adjacent normal tissues; **E–G** KM curves of high and low LRP2 expression in TCGA (**E**), GSE39582 (**F**), and GSE38832 (**G**). **H–K** The correlation of expression levels of LRP2 in COAD patients with pTNM stage (**H**), T stage (**I**), N stage (**J**), and M stage (**K**) in TCGA cohort. **** $P < 0.0001$

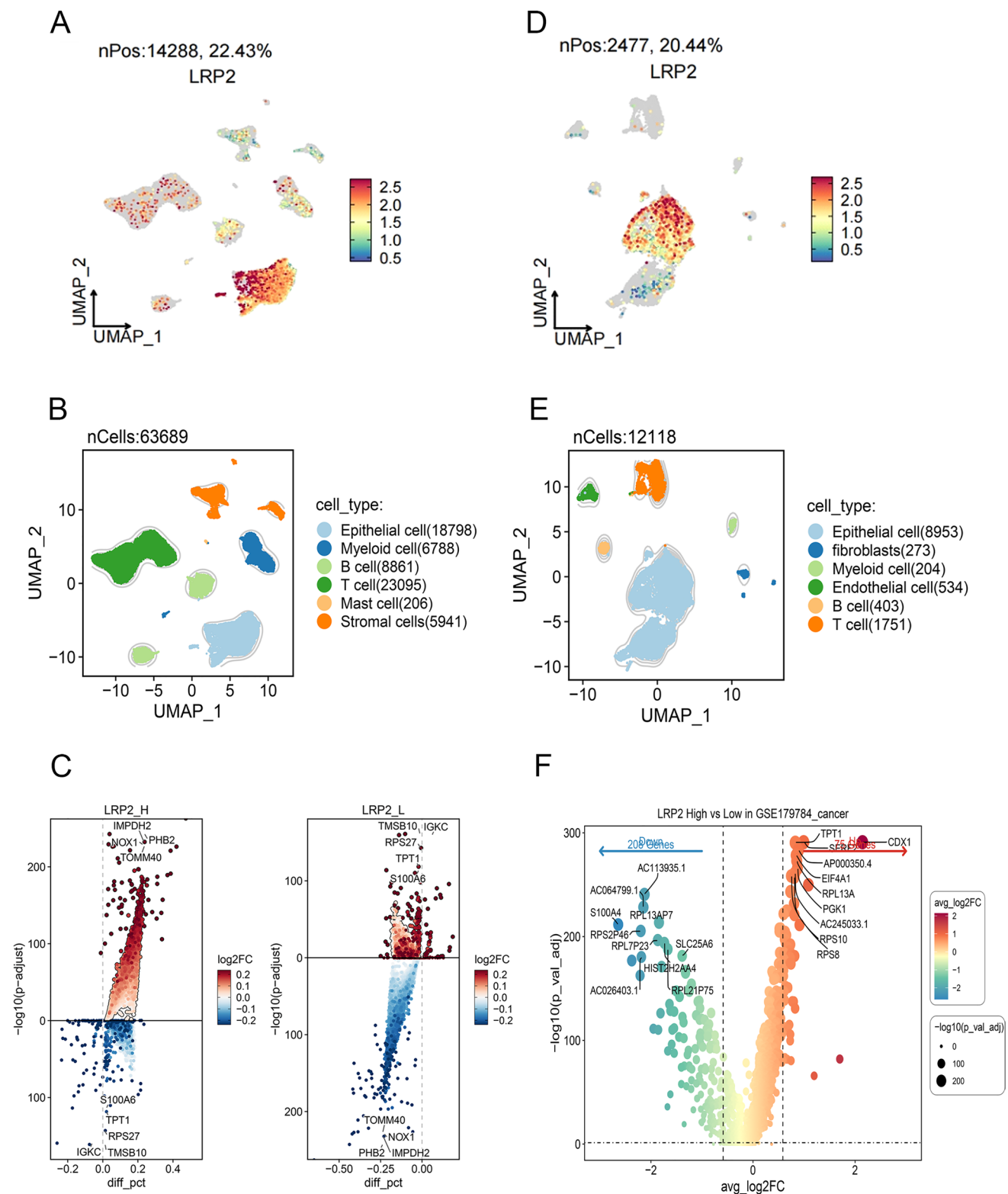


Fig. 4 Identification of cell subtypes and DEGs associated with LRP2 in the scRNA-seq data. **A** Eleven cell clusters were obtained applying the UMAP algorithm in GSE132465; **B** Six primary cell types were annotated by the given cell marker in GSE132465; **C** Differential expression genes of both higher and lower LRP2 expression groups in GSE132465; **D** Ten cell clusters were acquired using UMAP algorithm in GSE179784; **E** The annotation of 6 prominent cell types in GSE179784; **F** Volcano plot of diverse LRP2 levels in GSE179784

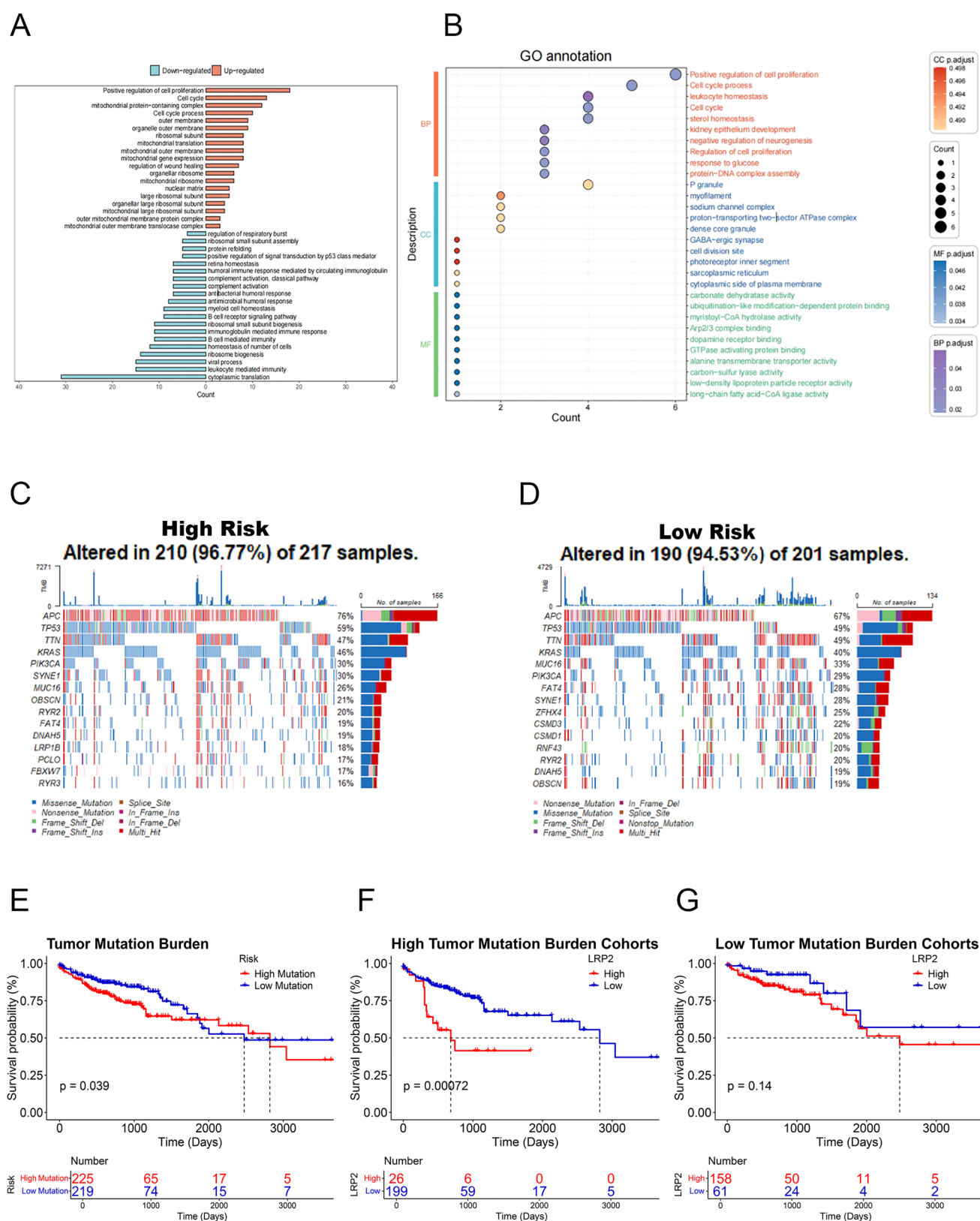


Fig. 5 GO analysis at single-cell sequencing level and TMB landscapes of LRP2. **A–B** GO annotation correlated with LRP2 in GSE132465 (**A**) and GSE179784 (**B**) datasets. **C** The waterfall plot of TMB in the high LRP2 expression cohort; **D** The landscapes portrayed the top 15 highly mutated genes in the low LRP2 expression group; **E** The KM curve of high and low TMB; **F–G** The KM plot related with LRP2 in high (**F**) and low (**G**) tumor mutation burden cohorts

model was evaluated executing ROC curves and the AUC figures of the construction model at 1, 3, and 5 years were 0.71, 0.722, and 0.757, respectively (Fig. 2F). We continued to apply GSEA analysis for investigating GO, KEGG and HALLMARK pathways to deeper understand the significance of these potential biomarkers in colon carcinoma occurrence and development. Some proliferation-related pathways were extensively enriched, including extracellular matrix structural constituent, GTPase activator activity, growth factor activity, growth cone, nuclear periphery, spindle, BMP signaling pathways, Wnt signaling pathways, calcium signaling pathway, Rap1 signaling pathway, cGMP-PKG signaling pathway, PI3K-Akt signaling pathway, MAPK signaling pathway, FoxO signaling pathway, myogenesis, hedgehog signaling, TNFA via NFkB signaling, G2M checkpoint and DNA repair, etc. (Fig. 2G, H and S1 F).

3.3 Evaluation between LRP2 expression level and prognosis of COAD patients

We preformed univariate Cox analysis aiming at 14 biomarkers obtained above again, and 9 signatures with crucially prognostic values were sieved from 379 colonic adenocarcinoma samples based on TCGA database ($P < 0.05$) (Fig. 3A). The multivariate Cox analysis displayed that both LRP2 (OR = 1.219, 95% CI: 1.069–1.389, $P = 0.00307$) and PPARGC1A (OR = 0.795, 95% CI: 0.707–0.893, $P = 0.00012$) might be utilized as independent factors of prognosis for COAD (Fig. 3B). Afterwards, 3 genes impacting patient survival were identified employing a univariate Cox regression analysis in GSE38832 ($P < 0.05$) (Fig. S1G). Interestingly, all of these genes including LRP2 (OR = 1.605, 95% CI: 1.045–2.465, $P = 0.03078$), CYP11A1 (OR = 1.450, 95% CI: 1.015–2.071, $P = 0.04097$) and PPARGC1A (OR = 1.219, 95% CI: 1.069–1.389, $P = 0.01036$) still behaved specific prognostic values in the multivariate Cox regression analysis ($P < 0.05$) (Fig. 3C). Compared to adjacent normal tissues, LRP2 was markedly upregulated, while the expression levels of CYP11A1 and PPARGC1A were fairly reduced in colon carcinoma samples ($P < 0.0001$) (Fig. 3D). CYP11A1 represented a positive association with an increased risk of colon cancer in GSE38832, but the same result was seemingly not obtained by multifactorial analysis in TCGA dataset. Moreover, the expression level of CYP11A1 was lessened in tumor samples, which signified it may not be an ideal prognostic marker. We continued to detect the prognostic evaluation roles of LRP2 and PPARGC1A in colon cancer patients.

From TCGA database (after excluding missing samples, 448 colon carcinoma samples remained), survival curve revealed that colon cancer patients with higher LRP2 expression had poorer prognoses ($P = 0.0017$) (Fig. 3E). In the GSE39582 dataset, colon cancer patients with LRP2 upregulation also exhibited significantly reduced survival time ($P = 0.046$) (Fig. 3F). In the GSE38832 database, LRP2 higher expression in colon cancer patients was also associated with momentarily worse prognosis ($P = 0.036$) (Fig. 3G). The ROC plot confirmed LRP2 owned an independent appraisal function, and the AUC values of LRP2 at 1, 2, and 3 years were 0.617, 0.628, and 0.648, respectively (Fig. S1H). Interestingly, PPARGC1A reflected an immensely opposite tendency that the incremental set could lengthen the survival rate in the TCGA ($P = 0.00042$), GSE39582 ($P = 0.23$), and GSE38832 ($P = 0.023$) (Fig. S2 A–C). It was reasonably speculated that two genes may be playing crucial roles in the progression of COAD, while we decided to pay attention to further investigate the relevant significance of LRP2 in regulating tumor status and prognosis assessment in COAD, due to its significantly elevated expression and high HR value in colon cancer tissues. To validate the prognostic value of LRP2 in colon cancer patients, we conducted a comprehensive analysis according to clinical features across various pathologic stages, N staging, M staging, T staging, gender, age, and CEA level in the disparate expression of LRP2 cohorts (Table S1).

LRP2 expression levels were strikingly associated with the pathologic stage ($P < 0.05$) (Fig. 3H), T stage ($P < 0.05$) (Fig. 3I), N stage ($P < 0.05$) (Fig. 3J), and M stage ($P < 0.05$) (Fig. 3K). Kaplan–Meier survival analyses revealed that the higher LRP2 expression group had worse overall survival compared to the lower group in different strata of clinical characteristics including stage II–IV, T2–T4, M0 or M1, and patients younger (<65 years) or older (≥ 65 years) (Fig. S2D–G). These results manifested that LRP2 possessed a prominent robustness for prognosis assessment of COAD.

3.4 scRNA-seq analysis unveiled the components of diverse cells and GO pathways contacted with LRP2 in COAD

After processing and refining the data, multitudinous expressions of marker genes were conducted to distinguish various cellular groupings in GSE132465 (Fig. 4A). After the tSEN and UMAP non-dimensionality carrying out strict quality control and filtration, a total of 63,689 cells were obtained. We identified 6 distinct cell subsets utilizing UMAP dimensionality reduction in GSE132465, including epithelial cell (18,798), myeloid cell (6788), B cell (8861), T cell (23,095), mast cell (206) and stromal cells (5941) (Fig. 4B). DEGs between high and low expression levels of LRP2 were displayed in the form of a volcano (Fig. 4C). Based on the annotation of known classical markers, 12, 118 cells were acquired in GSE179784 and 6 diverse cell types were categorized, which mainly concerned on epithelial cell (8953), fibroblasts (273), myeloid cell

Fig. 6 Analysis of GSEA, drug susceptibility, and immunohistochemical staining in different LRP2 expression groups. **A** GO pathways of GSEA for LRP2; **B** KEGG pathways of GSEA for LRP2; **C** Enrichment score of Wnt signaling pathway; **D** Drug susceptibility results; **E** Survival probability of clinical samples; **F** Immunohistochemical staining from collecting patient tissues

(204), endothelial cells (534), B cell (403) and T cell (1751) (Fig. 4D, E). We observed that 208 down-regulated and 75 up-regulated genes were identified in GSE179784 (Fig. 4F).

In the GO enrichment analysis through these DEGs, some proliferation-related pathways were prominently up-regulated in GSE132465, including positive regulation of cell proliferation, cell cycle, mitochondrial protein-containing complex, organelle outer membrane, mitochondrial translation, and regulation of wound healing (Fig. 5A). At the same time, we employed differentially expressed genes to conduct GO analysis in GSE179784. Concerning the BP, positive regulation of cell proliferation, cell cycle process, cell cycle, and sterol homeostasis contributed to tumor progression. Regarding CC, p granule, myofilament, GABA-ergic synapse, and cell division site were abundantly enriched. In terms of MF, carbonate dehydratase activity, myristoyl-CoA hydrolase activity, and GTPase activating protein binding were observed, separately (Fig. 5B). Therefore, we conjectured LRP2 might trigger colon carcinoma growth capacity according to the pathways associated with tumor germination.

3.5 Mutation profiles of COAD patients with different LRP2 expression levels

Genomic sequencing had fundamentally changed the understanding of somatic mutations in cancer, which would provide a detailed map of gene mutations and the processes driving cancer mutations [23]. Among the top 15 most frequently mutated genes, APC, TP53, TTN, KRAS, PIK3 CA, SYNE1, MUC16, OBSCN, RYR2, FAT4, and DNAH5 were shared high-frequency mutated genes across two groups, but the mutation frequencies of APC, TP53, KRAS, LRP1B, PCLO, FBXW7, and RYR3 were significantly increased in the high expression group (Fig. 5C, D). Surprisingly, the higher TMB tended to behave a worse OS compared with the lower TMB ($P = 0.039$) (Fig. 5E). Moreover, low expression of LRP2 group would reveal a better outcome compared with high expression group in high TMB subgroups ($P = 0.00072$) (Fig. 5F). The consistent results were represented in the low TMB cohorts, while without a statistically sufficient difference ($P = 0.14$) (Fig. 5G). The combination of LRP2 and TMB would represent nicely predictive prognosis values in COAD patients as well.

3.6 GSEA enrichment analysis of LRP2-related pathways in COAD

Differential analysis was implemented in colon cancer samples with different LRP2 expressions, which produced the identification of 430 DEGs (including 421 upregulated genes and 9 downregulated genes) (Fig. S3 A). GSEA was used to conduct GO, KEGG, and HALLMARK analyses to inspect the regulatory pathways of LRP2 in COAD. The results of the GO analysis indicated that LRP2 primarily participated in biological process (BP) such as epithelial to mesenchymal transition, developmental cell growth, BMP, Wnt, TGF- β , and notch signaling pathways. In cellular component (CC), it was mainly enriched in DNA packaging complex, growth cone, cullin-RING ubiquitin ligase complex, adherens junction, and mitotic spindle. In molecular function (MF), it was predominantly associated with extracellular matrix structural constituent, ATP-dependent activity, acting on DNA, helicase activity, cytoskeletal motor activity, and ATP hydrolysis activity (Fig. 6A).

According to KEGG pathway enrichment analysis, LRP2 may mainly be involved in the focal adhesion, transcriptional misregulation in cancer, Wnt, PI3K-Akt, mTOR, MAPK, cell cycle, and Rap1 signaling pathways (Fig. 6B). In the HALLMARK analysis, the signaling pathways were primarily enriched in Hedgehog signaling, angiogenesis, mitotic spindle, G2M checkpoint, TNFA/NFkB, E2 F targets, myogenesis and apical junction (Fig. S3B). Notably, both GO and HALLMARK enrichment analyses showed a high enrichment score for the Wnt signaling pathway and other proliferative pathways, and the Wnt enrichment plot was displayed in Fig. 6C.

Collectively, LRP2 certainly generated the energy to trigger the proliferative capability of COAD. Afterwards, we speculated that LRP2 may affect the progression of colon cancer modulating the Wnt pathway and further impact the prognosis of colon cancer patients.

3.7 Drug sensitivity analysis and immunohistochemical staining in COAD

Chemotherapy is one of the most significant treatment methods for colon cancer, and drug resistance remains a key research focus. Using the CellMiner database, we analyzed the complex relationship between LRP2 expression and

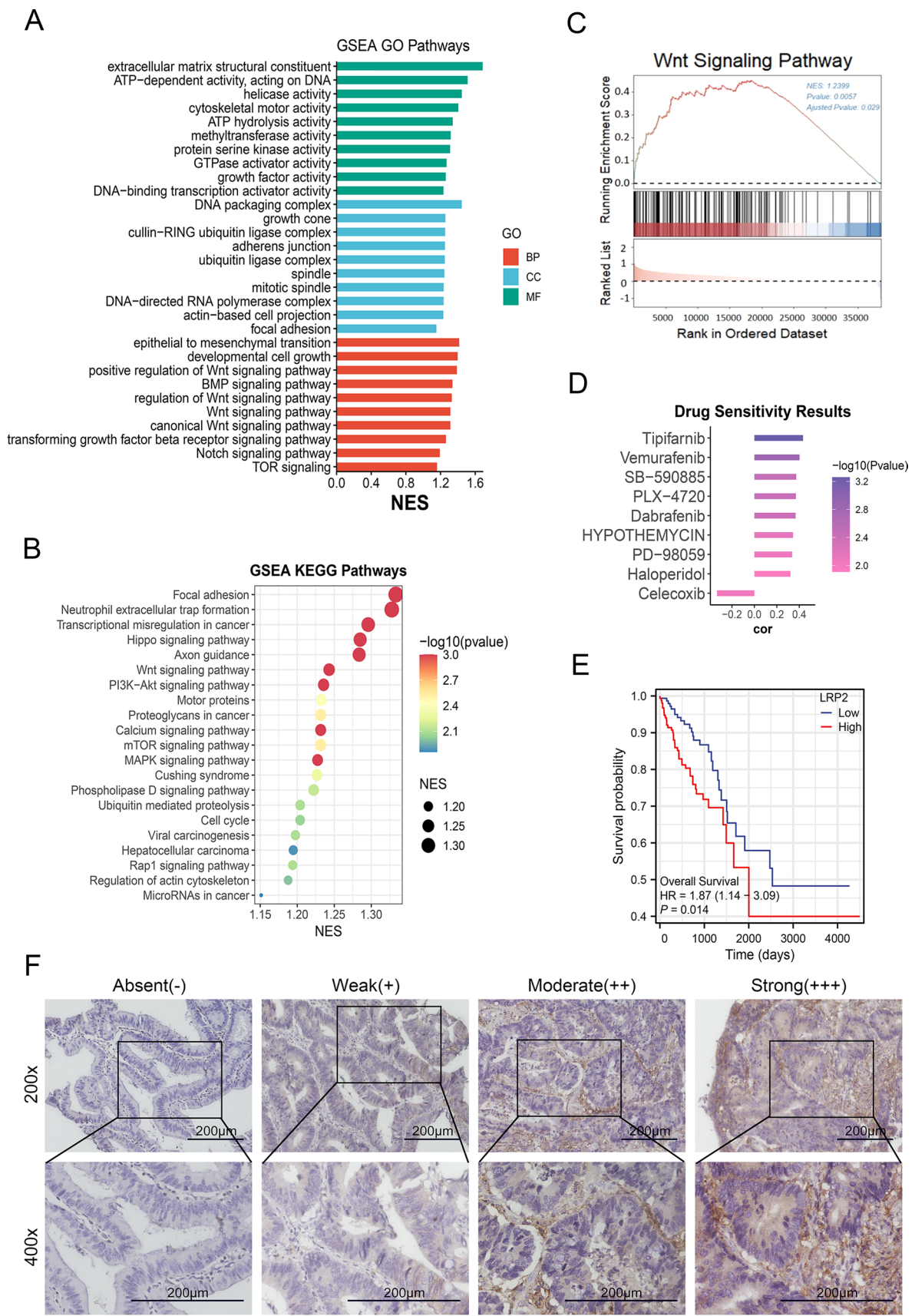


Fig. 7 LRP2 stimulated proliferative capability of HCT116 and SW480. **A** qPCR detection of LRP2 mRNA levels in HCT116 and SW480 overexpressed cell lines; **B** Western Blot estimation in two overexpression colon cancer cells; **C** CCK8 assay examined the proliferation ability of LRP2-OE colon cell lines; **D–E** EDU assay in overexpressed SW480 (**D**) and HCT116 (**E**); **F–G** Ki67 values in LRP2-overexpression SW480 (**F**) and HCT116 (**G**). **: $P < 0.01$; ***: $P < 0.001$; ****: $P < 0.0001$

cancer treatment drugs, revealing that high LRP2 expression was positively correlated with anti-cancer drugs, namely Tipifarnib, Vemurafenib, SB-590885, PLX-4720, Dabrafenib, Hypothemycin, PD-98059, and Haloperidol, and which indicated that high LRP2 expression generated colon carcinoma cells more sensitivities to these medications (Fig. 6D and S3 C–J). Conversely, the expression of LRP2 was negatively contacted with Celecoxib, suggesting a potential resistance with LRP2 expression arising (Fig. 6D and S3 K).

Additionally, immunohistochemistry analysis manifested the expression levels of LRP2 in colon cancer tissues were classified as 4 stages among different COAD patients, including absent, weak, moderate and strong (Fig. 6F). After integrating the clinical information about disparate patients, we found diminished expression of LRP2 could lengthen survival time contrasted with those patients of higher LRP2 expression ($P = 0.014$) (Fig. 6E). These results suggested that LRP2 would provide a striking insight for the clinical diagnosis and treatment of colon cancer.

3.8 LRP2 overexpression facilitated proliferative capacity of HCT116 and SW480 cell lines

Bioinformatics analysis unveiled that LRP2 was principally associated with multiple pathways promoting tumor cell proliferation, thereby impacting colon cancer progression. To verify the effect of LRP2 on the biological behavior of colon cancer cells, LRP2-overexpressing cell lines containing HCT116OE and SW480OE were constructed using lentiviral vectors in the colon cancer cell lines between HCT116 and SW480, respectively. Both qPCR detection and Western Blot assay results showed that the expression levels of LRP2 were significantly increased in the overexpression colon carcinoma cell lines ($P < 0.01$) (Fig. 7A, B).

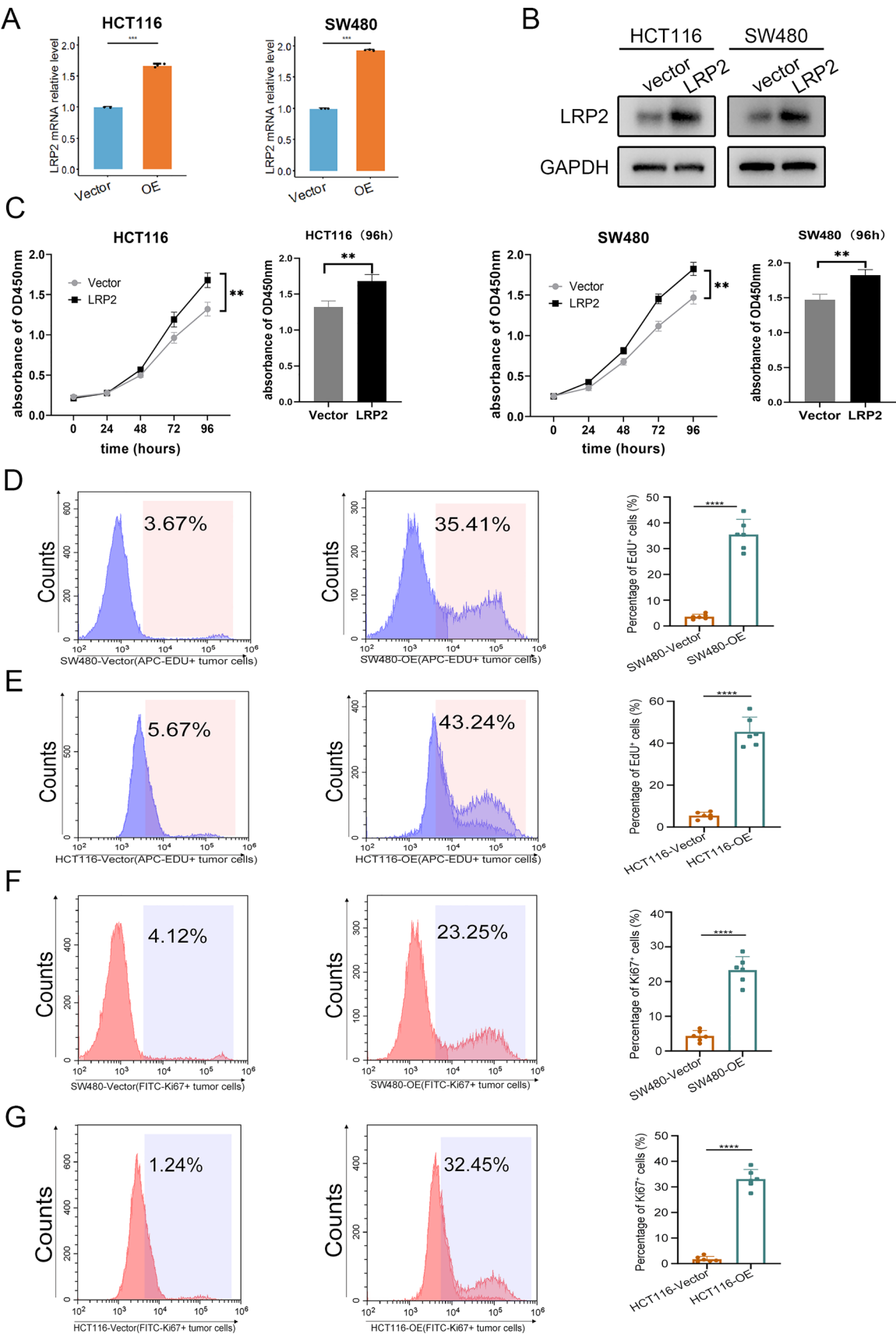
Subsequently, CCK-8 and flow cytometry assays were utilized to examine the effect of LRP2 overexpression on the proliferative capacity of HCT116 and SW480 cells. In the CCK-8 cell proliferation experiments, the OD values of HCT116 and SW480 cells with LRP2 overexpression were crucially upregulated ($P < 0.0001$) (Fig. 7C). Flow cytometry results also demonstrated that APC-EdU values extensively arose with the LRP2 overexpression in SW480 and HCT116 cell lines ($P < 0.0001$) (Fig. 7D, E). Consistently, the overexpression of LRP2 upgraded the percentage of FITC-Ki67 relative to the control of both two colon cancer cells (Fig. 7F, G). These results indicated that LRP2 overexpression might enforce the proliferation capacity of colon cancer cells.

4 Discussion

Colon cancer had become the third most common cancer globally and the second leading cause of death among cancer patients [24, 25]. In recent decades, the incidence of colorectal cancer in individual under 50 had significantly increased, with a considerable proportion of colorectal cancer patients being diagnosed with colon cancer [25, 26]. Approximately 15–30% of colon cancer patients experienced metastasis, and those with metastatic colon cancer had a poor prognosis, with a five-year survival rate being only 15% [27, 28]. Colon cancer continuously poses a threat to human health, particularly for younger populations, with its rising incidence and mortality rates requiring urgent attention. It was crucial to explore a biomarker that could monitor the progression of colon cancer and serve as a potential therapeutic target.

Metabolic reprogramming is a hallmark of tumor development. It not only represented the functional state of tumors but also played an assured role in the mechanisms underlying various cancers [29]. The Warburg effect described the abnormal aerobic glycolysis of malignant cells, which was the first discovery linking tumor biology with cell metabolism [30]. In recent years, the importance of mitochondrial-associated activities in the occurrence and development of tumors had gained increasing attentions [31].

We selected 31 mitochondria-related genes possessing clinical prognostic value by univariate Cox regression methods based on multi-omics data. These 31 prognostic-related genes were preformed consensus clustering analysis in TCGA and GEO datasets, and we observed that optimal clustering value occurred at $K = 2$. Survival analysis across the three datasets revealed that cluster 1 had a worse survival probability compared to cluster 2. Meanwhile, we constructed a risk assessment model through Lasso regression analysis and 14 important genes were identified, namely SMARCD3, ACBD4, MBOAT1, LRP2, OSBPL1A, PNPLA7, RAB6B, CYP11A1, TNFAIP8L3, ALOX12B, CHAT, SLCO1A2, ACSL6, and PPARGC1A. The



clinical prognosis assessment potentiality of COAD was further validated in utilizing two external validation cohorts. GSEA analysis of this model exerted partial biological effects on colon tumor. A significant enrichment of pathways related with tumor proliferation were observed, indicating that these gene sets might be helpful in facilitating carcinogenesis and growth. Undoubtedly, the Wnt signaling pathway was likewise noteworthy enrichment between GO and KEGG analysis. To further detect the crucial gene that occupied a well-established position in this gene set, we conducted multivariate Cox regression analysis and inferred that LRP2 played a striking role in the progression of colon cancer.

LRP2 was an important gene associated with mitochondrial metabolism, which was a multi-ligand endocytic receptor expressed in the apical membranes of various epithelial cells, including alveolar cells [32, 33], breast [34], thyroid [35], colon, prostate [36], and gallbladder [37] epithelial cells. LRP2 was a specific homodimer, which accelerated recycling to the cell surface from endosomes and enabled ligand to deliver and dissociate efficiently [15, 38]. This study confirmed the prognostic assessment value of mitochondrial metabolism-related genes in COAD through TCGA and GEO databases, discerning LRP2 as a crucial gene that may make a significant impact on the prognosis of COAD at the transcriptomic level. The study found that the expression of LRP2 was associated with the pathological staging of colon cancer, and high levels of LRP2 indicated a poor prognosis, suggesting that LRP2 may play a critical role in the development of colon cancer. In-depth research on LRP2 could assist to elucidate the pathogenesis of COAD.

With the advancements of single-cell technology, we obtained novel insights about tumor microenvironment and heterogeneity in CRC [39, 40]. In this study, to further investigate the prominent value of LRP2 in COAD, a total of 63,689 cells were acquired in the GSE132465 dataset, which was primarily classified into six categories based on marker gene sets. In the GSE179784, 6 major cell types were clustered similarly. Interestingly, the heterogeneity related to LRP2 was obvious in various cell types, with T cells displaying vitally assembled in GSE132465 and GSE179784. It was reported that single-track mitochondrial transportation occurred from T cells to neighboring cancer cells, checking the nanotube-based mutual effect between cancer and immune [41]. The mitochondria provided the essential energies for T cell activation and implicated it could further affect T cell dysfunction [42]. Simultaneously, it was recently observed cancer cells were metabolically empowered in the process of near-unidirectional mitochondrial transfer from T cells to tumor cells while immune cells were exhausted, supplying novel perspectives about immune evasion and tumor-T cell interaction [43]. In addition, an adequate number of patients were studied by mitochondrion transfer score, illustrating that mitochondrion transfer may produce a negative impact on patient survival by enhancing the proliferative ability of cancer cells [43]. Synthesizing these researches above and our study, it was reasonably supposed that mitochondrial function was positive with the dysfunction of T cells, resulting in the crumble of the cancer immune supervisory system. Collectively, LRP2, T cells, and mitochondria were inevitably connected, which required deeper research work to investigate.

We observed the biological roles of differential expression genes related with LRP2 by GO analysis from two single-cell sequencing datasets. These results exhibited that LRP2 might positively participate in mechanism regulation of cell proliferation, cell cycle, and GTPase activating protein binding, unraveling the LRP2 might play potential roles in accelerating colon tumor germination and development.

GSEA pathway enrichment analysis indicated that LRP2 was significantly enriched in pathways related to BMP, Wnt, TGF- β , Notch, TOR, Rap1, cGMP-PKG, PI3K-Akt, MAPK, cAMP, mTOR, Hedgehog, angiogenesis, mitotic spindle, and NF κ B/TNFA in colon cancer samples. The regulatory adaptation of cancer cells has been associated with various molecules metabolic activity, such as mTOR, AKT, Wnt, MAPK, and Notch [44–47].

These pathways were related to tumor progression regulation, where both GO and KEGG analyses showed the enrichment of the Wnt signaling pathway, indicating that LRP2 probably prompted tumor occurrence and germination, consistent with the findings that higher LRP2 level implicated a perishing prognosis in colon cancer. Interestingly, the Wnt signaling pathway had finished a noteworthy enrichment in the prognostic model, which underlined that LRP2 certainly occupies a commanding position synthesizing multivariate Cox regression analysis in the TCGA and GEO databases again. Drug sensitivity analysis represented high sensitivity to certain chemotherapy drugs with high expression of LRP2. These results suggested that LRP2 may be connected with the progression of colon cancer and could guide potential directions for cancer treatment.

In this immunohistochemical staining, the role of LRP2 was clearly demonstrated in dissimilar COAD tissue samples. The results manifested that high expression of LRP2 was a risk factor associated with poor prognosis in COAD patients. CCK-8 and flow cytometry assays indicated that LRP2 overexpression indeed enhanced the proliferative capacity of colon cancer cells, accordant with multi-omics analysis results. In cell experiments, we focused on LRP2 overexpressed cell lines, and established their direct connection with colon carcinoma cells. However, the uncertainty that LRP2 silencing cell lines would repress carcinogenesis and development of HCT116 and SW480 was reserved in this study. Moreover,

investigating how LRP2 modulates tumorigenesis in vivo and in vitro is mediated. Such as the potential involvement of cancer cell dissemination and progression in COAD and even other carcinomas, will be our future work.

Based on previous bioinformatics analyses regarding the relationship between LRP2 and COAD, several enrichment results displayed that LRP2 was likely to be involved in the regulation of the Wnt signaling pathway in colon carcinoma germination and progression. However, this inference should be validated through additional experimental studies. In future studies, we will continue to focus on exploring its potential mechanism in regulating metabolic activities and its clinical value as a therapeutic target in COAD. Certainly, we also expect more demanded findings interacted with this study would be replenished and further translated them into the solid clinical value to better serve COAD populations.

5 Conclusion

LRP2 established an impregnable relationship with gene mutations, prognosis, pathological stage, and susceptibility to anticancer drugs in COAD. LRP2 exactly participated in the regulation of multitudinous proliferative pathways based on single-cell sequencing and transcriptomics datasets. Enhanced expression levels of LRP2 would tend towards poor prognosis, which complemented novel perspectives for clinical diagnosis and treatment in COAD. LRP2 might strikingly accelerate the growth activity of HCT116 and SW480 cell lines.

Author contributions Jie Zhang and Xia Zhang designed the study; Jie Zhang and Yongjie Xie performed primary bioinformatic analyses and wrote the manuscript; Xiaobin Shang and Zhenyu Shi designed bioinformatic analyses and commented on the manuscript; Ziyun Liu and Xiaoqing Ma performed the cellular and immunohistochemical experiments; Jing Zhao designed the experiments employed in this study; Jie Zhang, Ziyun Liu and Xiaoqing Ma contributed to the collection of clinical samples. All authors reviewed the manuscript.

Funding Beijing-Tianjin-Hebei Basic Research Project of Tianjin Science and Technology Bureau (Grant Numbers: 22 JCZXJC00040); Public Health Science and Technology Major Project of the Tianjin Science and Technology Bureau (Grant Numbers: 21ZXGWSY00020); Tianjin Key Medical Discipline (Specialty) Construction Project (Grant Numbers: TJYXZDXK-011 A).

Data availability The datasets in this study can be publicly obtained from TCGA-COAD and GEO. The original contributions presented in the study are included in the article/Supplementary Material, further inquiries can be directed to the corresponding authors.

Declarations

Ethics approval and consent to participate All experimental protocols in this study were approved by the Ethics Committee of Tianjin Medical University Cancer Institute and Hospital. The authors affirm that all procedures contributing to this work comply with the ethical standards of relevant national and institutional committees on human experimentation.

Statement of compliance We hereby confirm that all methods employed in our project have been conducted in accordance with the relevant guidelines and regulations. We ensure that every aspect of our work adheres to established standards.

Competing interests The authors declare no competing interests.

Open Access This article is licensed under a Creative Commons Attribution-NonCommercial-NoDerivatives 4.0 International License, which permits any non-commercial use, sharing, distribution and reproduction in any medium or format, as long as you give appropriate credit to the original author(s) and the source, provide a link to the Creative Commons licence, and indicate if you modified the licensed material. You do not have permission under this licence to share adapted material derived from this article or parts of it. The images or other third party material in this article are included in the article's Creative Commons licence, unless indicated otherwise in a credit line to the material. If material is not included in the article's Creative Commons licence and your intended use is not permitted by statutory regulation or exceeds the permitted use, you will need to obtain permission directly from the copyright holder. To view a copy of this licence, visit <http://creativecommons.org/licenses/by-nc-nd/4.0/>.

References

1. Siegel RL, Wagle NS, Cercek A, Smith RA, Jemal A. Colorectal cancer statistics. *CA Cancer J Clin.* 2023;73(3):233–54.
2. Siegel RL, Miller KD, Jemal A. Cancer statistics. *CA Cancer J Clin.* 2020;70(1):7–30.
3. Biller LH, Schrag D. Diagnosis and treatment of metastatic colorectal cancer: a review. *JAMA.* 2021;325(7):669–85.
4. Argilés G, Tabernero J, Labianca R, Hochhauser D, Salazar R, Iveson T, Laurent-Puig P, Quirke P, Yoshino T, Taieb J, et al. Localised colon cancer: ESMO Clinical Practice Guidelines for diagnosis, treatment and follow-up. *Ann Oncol.* 2020;31(10):1291–305.
5. Hanahan D, Weinberg RA. Hallmarks of cancer: the next generation. *Cell.* 2011;144(5):646–74.

6. Marlein CR, Zaitseva L, Piddock RE, Robinson SD, Edwards DR, Shafat MS, Zhou Z, Lawes M, Bowles KM, Rushworth SA. NADPH oxidase-2 derived superoxide drives mitochondrial transfer from bone marrow stromal cells to leukemic blasts. *Blood*. 2017;130(14):1649–60.
7. Egan G, Khan DH, Lee JB, Mirali S, Zhang L, Schimmer AD. Mitochondrial and metabolic pathways regulate nuclear gene expression to control differentiation, stem cell function, and immune response in leukemia. *Cancer Discov*. 2021;11(5):1052–66.
8. Kolodziejczyk AA, Kim JK, Svensson V, Marioni JC, Teichmann SA. The technology and biology of single-cell RNA sequencing. *Mol Cell*. 2015;58(4):610–20.
9. Li J, Wu C, Hu H, Qin G, Wu X, Bai F, Zhang J, Cai Y, Huang Y, Wang C, et al. Remodeling of the immune and stromal cell compartment by PD-1 blockade in mismatch repair-deficient colorectal cancer. *Cancer Cell*. 2023;41(6):1152–1169.e1157.
10. Ohshima K, Oi R, Nojima S, Morii E. Mitochondria govern histone acetylation in colorectal cancer. *J Pathol*. 2021;256(2):164–73.
11. Chiang J-H, Tsai F-J, Hsu Y-M, Yin M-C, Chiu H-Y, Yang J-S. Sensitivity of allyl isothiocyanate to induce apoptosis via ER stress and the mitochondrial pathway upon ROS production in colorectal adenocarcinoma cells. *Oncol Rep*. 2020;44(4):1415–24.
12. Nykjaer A, Dragun D, Walther D, Vorum H, Jacobsen C, Herz J, Melsen F, Christensen EI, Willnow TE. An endocytic pathway essential for renal uptake and activation of the steroid 25-(OH) vitamin D3. *Cell*. 1999;96(4):507–15.
13. Barasch J, Hollmen M, Deng R, Hod EA, Rupert PB, Abergel RJ, Allred BE, Xu K, Darrah SF, Tekabe Y, et al. Disposal of iron by a mutant form of lipocalin 2. *Nat Commun*. 2016;7:12973.
14. Faber K, Hvidberg V, Moestrup SK, Dahlbäck B, Nielsen LB. Megalin is a receptor for apolipoprotein M, and kidney-specific megalin n-deficiency confers urinary excretion of apolipoprotein M. *Mol Endocrinol*. 2006;20(1):212–8.
15. Beenken A, Cerutti G, Brasch J, Guo Y, Sheng Z, Erdjument-Bromage H, Aziz Z, Robbins-Juarez SY, Chavez EY, Ahlsen G, et al. Structures of LRP2 reveal a molecular machine for endocytosis. *Cell*. 2023;186(4):821–836.e813.
16. He Y, Cao L, Wang L, Liu L, Huang Y, Gong X. Metformin inhibits proliferation of human thyroid cancer TPC-1 cells by decreasing LRP2 to suppress the JNK pathway. *Onco Targets Ther*. 2020;13:45–50.
17. Andersen RK, Hammer K, Hager H, Christensen JN, Ludvigsen M, Honoré B, Thomsen M-BH, Madsen M. Melanoma tumors frequently acquire LRP2/megalin expression, which modulates melanoma cell proliferation and survival rates. *Pigment Cell Melanoma Res*. 2015;28(3):267–80.
18. Meng C, Sun Y, Liu G. Establishment of a prognostic model for ovarian cancer based on mitochondrial metabolism-related genes. *Front Oncol*. 2023;13:1144430.
19. Vujkovic-Cvijin I, Sklar J, Jiang L, Natarajan L, Knight R, Belkaid Y. Host variables confound gut microbiota studies of human disease. *Nature*. 2020;587(7834):448–54.
20. Petegrosso R, Li Z, Kuang R. Machine learning and statistical methods for clustering single-cell RNA-sequencing data. *Brief Bioinform*. 2020;21(4):1209–23.
21. Subramanian A, Tamayo P, Mootha VK, Mukherjee S, Ebert BL, Gillette MA, Paulovich A, Pomeroy SL, Golub TR, Lander ES, et al. Gene set enrichment analysis: a knowledge-based approach for interpreting genome-wide expression profiles. *Proc Natl Acad Sci U S A*. 2005;102(43):15545–50.
22. Reinhold WC, Sunshine M, Liu H, Varma S, Kohn KW, Morris J, Doroshow J, Pommier Y. Cell Miner: a web-based suite of genomic and pharmacologic tools to explore transcript and drug patterns in the NCI-60 cell line set. *Cancer Res*. 2012;72(14):3499–511.
23. Martincorena I, Campbell PJ. Somatic mutation in cancer and normal cells. *Science*. 2015;349(6255):1483–9.
24. Sung H, Ferlay J, Siegel RL, Laversanne M, Soerjomataram I, Jemal A, Bray F: Global Cancer Statistics. GLOBOCAN estimates of incidence and mortality worldwide for 36 cancers in 185 countries. *CA Cancer J Clin*. 2020;71(3):209–49.
25. Ugai T, Sasamoto N, Lee H-Y, Ando M, Song M, Tamimi RM, Kawachi I, Campbell PT, Giovannucci EL, Weiderpass E, et al. Is early-onset cancer an emerging global epidemic? Current evidence and future implications. *Nat Rev Clin Oncol*. 2022;19(10):656–73.
26. Mutch MG. Molecular profiling and risk stratification of adenocarcinoma of the colon. *J Surg Oncol*. 2007;96(8):693–703.
27. Cervantes A, Adam R, Roselló S, Arnold D, Normanno N, Taïeb J, Seligmann J, De Baere T, Osterlund P, Yoshino T, et al. Metastatic colorectal cancer: ESMO clinical practice guideline for diagnosis, treatment and follow-up. *Ann Oncol*. 2023;34(1):10–32.
28. Dasari A, Lonardi S, García-Carbonero R, Elez E, Yoshino T, Sobrero A, Yao J, García-Alfonso P, Kocsis J, Cubillo Gracian A, et al. Fruquintinib versus placebo in patients with refractory metastatic colorectal cancer (FRESCO-2): an international, multicentre, randomised, double-blind, phase 3 study. *Lancet*. 2023;402(10395):41–53.
29. Martínez-Reyes I, Chandel NS. Cancer metabolism: looking forward. *Nat Rev Cancer*. 2021;21(10):669–80.
30. Hsu PP, Sabatini DM. Cancer cell metabolism: warburg and beyond. *Cell*. 2008;134(5):703–7.
31. Frattaruolo L, Brindisi M, Curcio R, Marra F, Dolce V, Cappello AR. Targeting the mitochondrial metabolic network: a promising strategy in cancer treatment. *Int J Mol Sci*. 2020;21(17):6014.
32. Buchäcker Y, Rummel S, Vohwinkel CU, Gabrielli NM, Grzesik BA, Mayer K, Herold S, Morty RE, Seeger W, Vadász I. Megalin mediates transepithelial albumin clearance from the alveolar space of intact rabbit lungs. *J Physiol*. 2012;590(20):5167–81.
33. Kolleck I, Sinha P, Rüstow B. Vitamin E as an antioxidant of the lung: mechanisms of vitamin E delivery to alveolar type II cells. *Am J Respir Crit Care Med*. 2002;166(12 Pt 2):S62–6.
34. Lundgren S, Carling T, Hjälmg G, Juhlin C, Rastad J, Pihlgren U, Rask L, Akerström G, Hellman P. Tissue distribution of human gp330/megalin, a putative Ca(2+)-sensing protein. *J Histochem Cytochem*. 1997;45(3):383–92.
35. Marinò M, Zheng G, McCluskey RT. Megalin (gp330) is an endocytic receptor for thyroglobulin on cultured fisher rat thyroid cells. *J Biol Chem*. 1999;274(18):12898–904.
36. Ternes SB, Rowling MJ. Vitamin D transport proteins megalin and disabled-2 are expressed in prostate and colon epithelial cells and are induced and activated by all-trans-retinoic acid. *Nutr Cancer*. 2013;65(6):900–7.
37. Erranz B, Miquel JF, Argraves WS, Barth JL, Pimentel F, Marzolo M-P. Megalin and cubilin expression in gallbladder epithelium and regulation by bile acids. *J Lipid Res*. 2004;45(12):2185–98.
38. Perez Bay AE, Schreiner R, Benedicto I, Paz Marzolo M, Banfelder J, Weinstein AM, Rodriguez-Boulán EJ. The fast-recycling receptor Megalin defines the apical recycling pathway of epithelial cells. *Nat Commun*. 2016;7:11550.
39. Ding J, Sharon N, Bar-Joseph Z. Temporal modeling using single-cell transcriptomics. *Nat Rev Genet*. 2022;23(6):355–68.

40. Zhang Y, Song J, Zhao Z, Yang M, Chen M, Liu C, Ji J, Zhu D. Single-cell transcriptome analysis reveals tumor immune microenvironment heterogeneity and granulocytes enrichment in colorectal cancer liver metastases. *Cancer Lett.* 2020;470:84–94.
41. Saha T, Dash C, Jayabalan R, Khiste S, Kulkarni A, Kurmi K, Mondal J, Majumder PK, Bardia A, Jang HL, et al. Intercellular nanotubes mediate mitochondrial trafficking between cancer and immune cells. *Nat Nanotechnol.* 2021;17(1):98–106.
42. Desdín-Micó G, Soto-Herederó G, Mittelbrunn M. Mitochondrial activity in T cells. *Mitochondrion.* 2018;41:51–7.
43. Zhang H, Yu X, Ye J, Li H, Hu J, Tan Y, Fang Y, Akbay E, Yu F, Weng C, et al. Systematic investigation of mitochondrial transfer between cancer cells and T cells at single-cell resolution. *Cancer Cell.* 2023;41(10):1788–1802.e1710.
44. Fei X, Huang J, Li F, Wang Y, Shao Z, Dong L, Wu Y, Li B, Zhang X, Lv B, et al. The Scap-SREBP1-S1P/S2P lipogenesis signal orchestrates the homeostasis and spatiotemporal activation of NF- κ B. *Cell Rep.* 2023;42(6):112586.
45. Glaviano A, Foo ASC, Lam HY, Yap KCH, Jacot W, Jones RH, Eng H, Nair MG, Makvandi P, Geoerger B, et al. PI3K/AKT/mTOR signaling transduction pathway and targeted therapies in cancer. *Mol Cancer.* 2023;22(1):138.
46. Zhao H, Ming T, Tang S, Ren S, Yang H, Liu M, Tao Q, Xu H. Wnt signaling in colorectal cancer: pathogenic role and therapeutic target. *Mol Cancer.* 2022;21(1):144.
47. Ponsioen B, Post JB, Buissant des Amorie JR, Laskaris D, van Ineveld RL, Kersten S, Bertotti A, Sassi F, Sipietier F, Cappe B, et al. Quantifying single-cell ERK dynamics in colorectal cancer organoids reveals EGFR as an amplifier of oncogenic MAPK pathway signaling. *Nat Cell Biol.* 2021;23(4):377–90.

Publisher's Note Springer Nature remains neutral with regard to jurisdictional claims in published maps and institutional affiliations.